

Emission of nitrous acid from soil and biological soil crusts represents an important source of HONO in the remote atmosphere in Cyprus

Hannah Meusel¹, Alexandra Tamm¹, Uwe Kuhn¹, Dianming Wu^{1, #}, Anna Lena Leifke¹, Sabine Fiedler², Nina Ruckteschler¹, Petya Yordanova¹, Naama Lang-Yona¹, Mira Pöhlker¹, Jos Lelieveld^{3, 4}, Thorsten Hoffmann⁵, Ulrich Pöschl¹, Hang Su^{6, 1}, Bettina Weber¹, Yafang Cheng^{1, 6}

¹Max Planck Institute for Chemistry, Multiphase Chemistry Department, Mainz, Germany

²Johannes Gutenberg University, Institute for Geography, Mainz, Germany

³Max Planck Institute for Chemistry, Atmospheric Chemistry Department, Mainz, Germany

⁴The Cyprus Institute, Nicosia, Cyprus

⁵Johannes Gutenberg University, Institute for Inorganic and Analytical Chemistry, Mainz, Germany

⁶Institute for Environmental and Climate Research, Jinan University, Guangzhou, China

[#]now at: School of Geographic Sciences, East China Normal University, Shanghai, China

Corresponding author: Hang Su (h.su@mpic.de) and Bettina Weber (b.weber@mpic.de)

Abstract. Soil and biological soil crusts can emit nitrous acid (HONO) and nitric oxide (NO). The terrestrial ground surface in arid and semi-arid regions is anticipated to play an important role in the local atmospheric HONO budget, deemed to represent one of the unaccounted HONO sources frequently observed in field studies. In this study HONO and NO emissions from a representative variety of soil and biological soil crust samples from the Mediterranean island Cyprus were investigated under controlled laboratory conditions. A wide range of fluxes was observed, ranging from 0.6 to 264 ng m⁻² s⁻¹ HONO-N at optimal soil water content (20-30% of water holding capacity, WHC). Maximum NO-N fluxes at this WHC were lower (0.8-121 ng m⁻² s⁻¹). Highest emissions of both reactive nitrogen species were found from bare soil, followed by light and dark cyanobacteria-dominated biological soil crusts (biocrusts), correlating well with the sample nutrient levels (nitrite and nitrate). Extrapolations of lab-based HONO emission studies agree well with the unaccounted HONO source derived previously for the extensive CYPHEX field campaign, i.e., emissions from soil and biocrusts may essentially close the Cyprus HONO budget.

1 Introduction

Nitrous acid (HONO) plays an important role in tropospheric chemistry, as it is one of the major precursors of the hydroxyl (OH) radical which determines the oxidizing capacity of the atmosphere. In the early morning, HONO photolysis has been shown to contribute up to 30% to the local OH budget (Alicke et al., 2002; Kleffmann et al., 2005; Ren et al., 2003 and 2006; Meusel et al., 2016). Currently, the HONO formation processes, especially during daytime, are still not fully understood. Recent ground based field measurements showed unexpected high daytime concentrations of HONO, which could not be solely explained by atmospheric gas phase reactions (R1-R3) (Kleffmann et al., 2003 and 2005; Su et al., 2008a; Sörgel et al., 2011a; Su et al., 2011; Michoud et al., 2014; Czader et al., 2012; Wong et al., 2013; Tang et al., 2015; Oswald et al., 2015; Meusel et al., 2016).





Several studies have shown that HONO can be heterogeneously formed from NO₂ on a variety of surfaces, e.g., soot, humic acid, minerals, proteins and organically coated particles (Ammann et al., 1998; Arens et al., 2001; Aubin et al., 2007; Bröske et al., 2003; Han et al., 2013; Kalberer et al., 1999; Kleffmann et al., 1999; Kleffmann and Wiesen, 2005; Lelievre et al., 2004; Kinugawa et al., 2011; Liu et al., 2015; Wang et al., 2003; Yabushita et al., 2009; Meusel et al., 2017). Light can activate some of these surfaces (humic acid, proteins and other organic compounds, titanium dioxide, soot), which enhances NO₂ uptake and HONO production (George et al., 2005; Langridge et al., 2009; Monge et al., 2010; Ndour et al., 2008; Ramazan et al., 2004; Stemmler et al., 2007; Kebede et al., 2013; Meusel et al., 2017). But NO₂ uptake coefficients and the ambient aerosol surface areas for heterogeneous reactions of NO₂ were nevertheless frequently found to be too low to account for the observed HONO production rates (Stemmler et al., 2007; Sarwar et al., 2008; Zhang et al., 2016). Besides the heterogeneous NO₂ reaction, Bejan et al. (2006) observed HONO formation during irradiation of nitrophenols. Photolysis of nitrate or nitric acid generates HONO as well (Baergen and Donaldson, 2013; Scharko et al., 2014; Zhou et al., 2003, 2011). Contrary to the detected missing HONO source near the ground, recent airborne measurements (500-1200 m above ground level) observed HONO concentrations, which could be explained by gas phase reactions only (Li et al., 2014; Neuman et al., 2016). However, vertical gradient studies showed higher HONO concentrations near the ground than in higher altitudes indicating a ground level source (Harrison and Kitto, 1994; Kleffmann et al., 2003; Ren et al., 2011; Stutz et al., 2002; VandenBoer et al., 2013; Villena et al., 2011; Zhou et al., 2011; Wong et al., 2012 and 2013; Vogel et al., 2003; Zhang et al., 2009; Young et al., 2012). This is supported by gas exchange studies showing that HONO and NO can be emitted from (natural) soil and biological soil crusts (biocrusts, BSC), even without applying atmospheric NO₂ (Su et al., 2011; Oswald et al., 2013; Mamtimin et al., 2016; Weber et al., 2015; Meixner and Yang, 2006). HONO and NO can be formed during biological processes (nitrification and denitrification; Pilegaard, 2013), in which NH₃ or NH₄⁺ is oxidized stepwise or NO₃⁻ is reduced (Fig. 1). Depending on soil-pH and according to Henry's law soil nitrite (NO₂⁻) can be converted into gaseous HONO. It was found that sterilized soil emit lower amounts of reactive nitrogen than natural soil (Oswald et al., 2013; Weber et al., 2015).

Biocrusts grow within the uppermost millimeters to centimeters of soil in arid and semi-arid ecosystems. They are composed of photoautotrophic cyanobacteria, algae, lichens, and bryophytes, growing together with heterotrophic bacteria, fungi and archaea in varying proportions (Belnap et al., 2016). Depending on the dominating photoautotrophs, cyanobacteria-dominated biocrusts with an initial thin light-colored and a well-developed dark type, cyanolichen- and chlorolichen-dominated biocrusts with lichens comprising cyanobacteria or green algae as photobionts, and bryophyte-dominated biocrusts are distinguished (Büdel et al., 2009). Many free living cyanobacteria but also those in symbiosis with fungi (forming lichens) and vascular plants can fix atmospheric nitrogen N₂ and convert it into ammonia (Cleveland et al., 1999; Belnap 2002; Herridge et al., 2008; Barger et al., 2016). Globally it has been estimated that 100-290 Tg (N) yr⁻¹ is fixed biologically (Cleveland et al., 1999), of which 49 Tg yr⁻¹ (17-49%) is fixed by cryptogamic covers, which comprise biocrusts, but also other microbially dominated biomes, like lichen and bryophyte communities occurring on soil, rocks and plants in boreal and tropical regions (Elbert et al., 2012). Studies have suggested, that nitrogen cycling in soil (N₂ fixation, nitrification, denitrification)

and hence reactive nitrogen emission (NO , N_2O , HONO) is often enhanced by well-established biocrusts, especially by dark cyanobacteria (Cleveland et al., 1999; Elbert et al., 2012; Belnap, 2002; Barger et al., 2013; Johnson et al., 2005; Abed et al., 2013; Strauss et al., 2012; Weber et al., 2015). But much of the molecular biology/chemistry that is important for atmosphere-land interactions is likely occurring just below the crust (that is visible at the surface). In Cyprus, an island in the semi-arid eastern Mediterranean area, biocrusts are ubiquitously covering ground surfaces and hence can be anticipated to play an important role in the local HONO budget. In the CYPHEX campaign 2014 (CYprus PHotochemical EXperiment) the observed diel cycles of HONO ambient air concentrations revealed strong unaccounted sources of HONO and NO , being well correlated with each other (Meusel et al., 2016). With low NO_2 concentrations and high HONO/NO_x ratios, respectively, direct emissions from combustion and heterogeneous reactions of NO_2 could be excluded as significant HONO sources, leaving emissions from soil and the respective surface cover to be the most plausible common source for both nitrogen species (Meusel et al., 2016). In the present study we have measured HONO and NO fluxes from soil and biocrust samples from Cyprus by means of a dynamic chamber system. The aim of this study was to characterize and quantify direct trace gas emissions and demonstrate their impact on the atmospheric chemistry in the remote coastal environment of Cyprus.

2 Methods

2.1 Sampling

Bare soil and biocrust samples were collected on 27th April 2016 on the South/South-East side of the military station in Ineia, Cyprus (34.9638°N, 32.3778°E), where the CYPHEX campaign took place in 2014. It is a rural site about 600 m above sea level (asl), approximately 5-8 km from the coast and is surrounded by typical Mediterranean vegetation (olive and pine trees, small shrubs like *Pistacia lentiscus*, *Sacopoterium spinosum* and *Inula viscosa*). More details about the site can be found in Meusel et al. (2016).

In an area of about 8580 m² (South/South-East direction of the station) 50 grids (25x25 cm) were placed at randomly selected spots for systematic ground cover assessment. At each grid point occurrence of nine types of surface cover (i.e., light and dark cyanobacteria-, chlorolichen-, cyanolichen-, and moss-dominated biocrust, bare soil, stone, litter, vascular vegetation/shrub) were assigned and quantified. Spatially independent replicate samples were collected of light cyanobacteria-dominated biocrusts (light BSC), dark cyanobacteria-dominated biocrusts with cyanolichens (dark BSC), chlorolichen-dominated biocrusts (chlorolichen BSC I, chlorolichen BSC II), moss-dominated biocrusts (moss BSC) and of bare soil (Fig. S1 of the supplement). Each sample was collected in dry state in a plastic petri dish (diameter 5.5. cm, height 1 cm), sealed and stored in the dark at room temperature until further analysis (storage time less than 15 weeks). Based on previous experiments in our laboratory, it can be anticipated that the sample's chemical (nutrient content) and biological (chlorophyll content) properties were not deteriorated during storage (a manuscript on this study will be submitted soon). In total 43 samples were collected (Table 1) of which 18 samples, i.e., 3 replicates of each HONO emitting surface cover type were used directly (upfront) for nutrient analysis, while all others were first used for trace gas exchange measurements, prior to nutrient and chlorophyll content analysis.

2.2 Meteorological data

During CYPHEX the meteorological parameters were measured at about 5 m above ground, considered not representative for the micro-habitat of the soil ground surface. Hence we placed three humidity (and temperature) sensors (HOBO Pro v2) just on top of the soil surface about 4 weeks prior to sample collection. Reference meteorological data (air temperature, humidity and precipitation) from Paphos airport (about 20 km south of the sample area, 12 m asl) and Prodromos (about 40 km east of the sampling area, 1380 m asl) during the sampling period as well as the precipitation data from the last 4 years (2013-2016) were provided by the Department of Meteorology, Cyprus (http://www.moa.gov.cy/moa/ms/ms.nsf/DMLmeteo_reports_en/MLmeteo_reports_en?opendocument; last access: Dec. 2016).

2.3 Soil characteristics: nutrient, chlorophyll and pH

Soil characteristics (nutrient, pH) have an effect on soil emission, e.g., higher nutrient level and lower pH would enhance emission according to Henry law (Su et al., 2011). Nutrient analysis was conducted on samples without gas exchange measurements ($n = 3$) and on replicate samples after gas exchange measurements in order to analyze potential effects of the applied 'wetting-drying' cycle. Nitrate (NO_3^-), nitrite (NO_2^-) and ammonium (NH_4^+) were analyzed via flow injection analysis with photometric detection (FIAstar 5000, Foss, Denmark). Prior to that, the samples comprised of soil and its biocrust-cover were gently ground and an aliquot of 7 g was solved in 28 mL of 0.0125 M CaCl_2 . After shaking for 1 hour the mixture was filtered on a N-free filter. The detection limits were 0.014, 0.046 and 0.047 mg kg^{-1} for NO_2^- -N, NO_3^- -N and NH_4^+ -N, respectively.

Chlorophyll analysis, as an indicator of biomass of photo-autotrophic organisms, was done according to the dimethyl sulfoxide (DMSO) method (Ronen and Galun, 1984). Ground samples were extracted twice with CaCO_3 saturated DMSO (20 mL, 10 mL) at 65°C for 90 min. Both extracts were combined and centrifuged (3000 G) at 15°C for 10 min. The light absorption at 648, 665 and 700 nm was detected with a spectral photometer (Lambda 25 UV/VIS Spectrometer, Perkin Elmer, Rodgau). The amount of chlorophyll a (Chl_a) was calculated according to Arnon et al. (1974). Chlorophyll a+b (Chl_{a+b}) content was calculated according to Lange, Bilger and Pfanz (pers. comm. in Weber et al., 2013):

$$\text{Chl}_{a+b}[\mu\text{g}] = (20.2 \cdot (E_{648} - E_{700}) + 8.02 \cdot (E_{665} - E_{700})) \cdot a \quad (\text{eq.1})$$

$$\text{Chl}_a[\mu\text{g}] = (12.19 \cdot (E_{665} - E_{700})) \cdot a \quad (\text{eq.2})$$

where $\text{Chl}_{a+b}[\mu\text{g}]$, $\text{Chl}_a[\mu\text{g}]$ is the chlorophyll content of the sample, E_{648} , E_{665} , E_{700} are light absorption at the given wavelength, and a is the amount of DMSO used in mL.

The pH was determined for each surface cover type ($n = 3-4$) according to Weber et al. (2015, Suppl.). Here, 1.5 g of the ground sample was mixed with 3.75 mL of pure water and shaken for 15 min. Then the slurry was centrifuged (3000 G, 5 min) to separate the solid phase from the liquid solution. The latter was used for pH determination by means of a pH electrode (Inlab Export Pro-ISM, Mettler Toledo).

2.4 Trace gas exchange measurements

The dynamic chamber method for analyzing NO and HONO emissions from soil samples was already introduced before (Oswald et al., 2013; Weber et al., 2015; Wu et al., 2014) and in general showed good agreement with flux

measurements in the field (van Dijk et al., 2002; Rummel et al., 2002). Intact soil and biocrust samples (25-35 g in a plastic petri dish with 5.5 cm diameter and about 1 cm height) were wetted with 8-13 g of pure water (18.2 MΩ) up to full water holding capacity and placed into a dynamic Teflon film chamber (≈ 47 L) flushed with 8 L min⁻¹ dry pure air (PAG 03, Ecophysics, Switzerland). Intact (biocrust) samples consist of a few mm of the biocrust and the underlying soil. Typical drying cycles lasted between 6 and 8 hours. A Teflon coated internal fan ensured complete mixing of the chamber headspace volume. During the experiments the chamber was kept at constant temperature (25°C, the mean daytime air temperature during CYPHEX) and in darkness to avoid photochemical reactions. At the chamber outlet the emitted gases HONO, NO and water vapor were quantified. HONO was analyzed with a commercial long path absorption photometer (LOPAP, QUMA GmbH; Wuppertal, Germany), with a detection limit of ~ 4 ppt and 10% uncertainty (based on the uncertainties of liquid and gas flow, concentration of calibration standard and regression of calibration). To avoid any transformation of HONO in the tubing, the sampling unit including the stripping coil from LOPAP was directly connected to the chamber. NO_x (NO + NO₂) was detected with a commercial chemiluminescence detector (42i TL, Thermo Scientific; Waltham, USA) modified with a photolytic converter with a detection limit of ~ 50 ppt (NO) and ~ 200 ppt (NO₂). An infrared CO₂ and H₂O analyzer (Li-840A, LICOR; Lincoln, USA) was used to log the drying and to calculate the soil water content (SWC) of the samples as follows:

$$SWC(WHC) = \frac{m_{H_2O,t=n}}{m_{H_2O,0}} * 100 \quad (\text{eq. 3})$$

$$m_{H_2O,t=n} = m_{H_2O,t=n-1} - \frac{S_{Licor,t=n}}{\sum_{t=0}^{t=N} S_{Licor}} * m_{H_2O,0} \quad (\text{eq. 4})$$

with t=0 denoting the measurement start (wetted sample inserted into chamber), t=n: any time between 0 and N, t=N: time when sample had dried out and measurement was stopped, S_{Licor}: absolute H₂O signal at a given time, m_{H₂O,0}: mass of water added to sample (water holding capacity, WHC), SWC: soil water content in % WHC.

2.5 Data analysis

Measured data of NO₂⁻, NO₃⁻, NH₄⁺, Chl_{a+b}, Chl_a, NO and HONO optimum flux and NO and HONO integrated flux did not follow a normal distribution. Rather, log-transformed data were normally distributed (Shapiro-Wilk) and therefore used for statistical analysis (Pearson correlation, ANOVA including Tukey Test with significance level of p = 0.05) executed with OriginPro (version 9.0; OriginLab corporation, Northampton, Massachusetts, USA).

Precipitation data from the last 4 years (2013-2016), provided by the Department of Meteorology of Cyprus, indicating about 30 rain events per year (precipitation > 1 mm with following one or more dry days) were used to estimate annual emissions of total nitrogen in terms of HONO and NO.

3 Results and discussion

3.1 Meteorological conditions

One month before sampling, three sensors measuring temperature and relative humidity were installed directly above the soil surface in the field to represent the micro-climate of the ground surface. Reference air temperature, humidity and precipitation measurements at Paphos airport and Prodromos showed one rain event on 11-12 April which is

reflected by higher soil humidity (80-100%) and lower temperatures on these days (see Fig. S2). As a consequence, the biological soil crusts were activated and went through one full wetting and drying cycle before sample collection. Temperature above the soil ranged from 10°C in the night to 50°C during the day when solar radiation was most intense. Air temperature was similar during the night but not as hot during the day ranging between 20° and 30°C. Humidity above the ground was low during daytime (<30% rH) and increased during the night up to 80%, while the atmospheric relative humidity (at Paphos airport) ranged between 47 and 73% (without rain event). Thus there were only little variations of humidity with height above the soil surface. Above the ground surface the relative humidity was somewhat lower during the day (mainly caused by higher temperatures) but somewhat higher during the night, compared to respective weather station data. During and shortly after the main rain event humidity at ground level was higher (80 and 100% rH) compared to ambient air humidity (70-85% rH). Ambient air temperatures were somewhat lower during sample collection of this study as compared to the CYPHEX field campaign in 2014. During CYPHEX, nighttime temperatures (3 m above ground level) did not drop below 18°C. Relative humidity (3 m above ground level) was mostly between 70 and 100% with only two short periods with humidity between 20-60% rH. Hence we can assume that soil surface temperatures were higher and ground rH in the same range during CYPHEX compared to sampling period.

3.2 Cyprus soil and biocrust characteristics

The different biocrust types were distinguished in the field based on the dominating phototrophic compound but which provides no information about the microbial community below or about the magnitude of (de)nitrification processes. The microbial community couldn't be determined by non-destructive methods. Systematic mapping of surface covers revealed that moss-dominated biocrusts are the most frequent in the investigated Cyprus field site area (21.3%), followed by light (10.4%) and dark BSC (6.5%), whereas chlorolichen- (3.2%) and cyanolichen-dominated BSC (1.8%) only played a minor role (Fig. 2, Fig. S1). The soil surface was partially covered by litter (26.3%), stones (19.5%) and vascular vegetation (8.5%), whereas open soil was rarely found (2.5%). It was previously established that soil and biocrusts emit HONO and NO (Weber et al., 2015; Oswald et al., 2013), jointly accounting for 45.6% of surface area in our studied region. To the best of our knowledge, no data on reactive nitrogen emissions from vascular vegetation and plant litter have been published yet.

Nutrient analysis revealed large variations in concentrations of nitrogen species ranging from 0 to 6.48, 0 to 0.57 and 0 to 22.2 mg (N) kg⁻¹ of dry soil/crust mass for NO₃⁻, NO₂⁻, and NH₄⁺, respectively (Fig. 3a, Tab. S1 of the supplement). In general, no significant change in reactive nitrogen contents was found before and after the trace gas exchange experiments, indicating no significant impact of one wetting-drying cycle on the nutrient content. Bare soil samples had significantly higher levels of NO₃⁻ and NO₂⁻ content compared to dark, chlorolichen and moss BSC. Among the latter three, no significant differences in nutrient levels were observed. Light BSC had NO₂⁻ contents similar to bare soil. The NH₄⁺ content was very similar in all samples, except for one outlier in the group of light BSC with strongly elevated NH₄⁺. Higher nitrate and ammonium levels in bare soil compared to crust-covered samples were also reported recently for a warm desert site in South Africa (Weber et al., 2015), indicative of nutrient consumption/integration by the biocrusts. Nitrite, on the other hand, was lower for bare soil samples compared to

biocrust samples. While NO_3^- was slightly higher, NH_4^+ and NO_2^- contents (especially of bare soil samples) were lower in the South African arid ecosystem compared to Cyprus.

Chlorophyll was only determined in the samples used for flux measurements. Chl_a ranged from 4.1 (bare soil) to 144.2 mg m^{-2} (moss BSC) and Chl_{a+b} from 9.3 (bare soil) to 211.3 mg m^{-2} (moss BSC), respectively (Fig. 3b, Tab. S1). From bare soil, via light BSC and chlorolichen BSC II, to dark BSC the chlorophyll content increased, but not significantly ($p > 0.2$). Nevertheless, Chl_a and Chl_{a+b} contents of chlorolichen BSC I and moss BSC were significantly higher than these of bare soil, light BSC and chlorolichen BSC II ($p < 0.05$, Fig. 43). The range of chlorophyll contents is comparable to previous arid ecosystem studies (Weber et al., 2015).

The pH of soil and biocrusts ranged between slightly acidic (6.2) and slightly alkaline (7.6; Fig. 3c). The mean pH of 17 samples was 7.0, i.e., neutral. Only the pH of moss BSC samples was significantly lower than that of bare soil, light BSC and chlorolichen BSC samples ($p = 0.05$). Soil and biocrust samples from South Africa were slightly more alkaline (7.1-8.2) with no significant difference among biocrust types (Weber et al., 2015).

3.3 NO and HONO flux measurements

All samples showed HONO and NO emissions during full wetting and drying cycles. The calculations of the emission or flux rates are shown in the supplement. Maximum emission rates of HONO were observed at about 17-33% WHC, and of NO at 20-36% with no significant differences between all soil cover types (Fig 4). Emissions declined to zero at 0% WHC and to very small rates for >70%. Emission maxima strongly varied between soil cover types, but also between samples of the same cover type (see Fig. 4 and 5, and Table S1). Highest emissions of both HONO-N and NO-N were detected for bare soil (175 ± 50.4 and $92.2 \pm 20.0 \text{ ng m}^{-2} \text{ s}^{-1}$; values indicate mean \pm standard error), followed by light (48.6 ± 24.3 and $44.0 \pm 22.4 \text{ ng m}^{-2} \text{ s}^{-1}$) and dark BSC (27.1 ± 16.1 and $26.5 \pm 15.9 \text{ ng m}^{-2} \text{ s}^{-1}$). Both types of chlorolichen- and moss-dominated biocrusts showed very low emission rates of reactive nitrogen (on average $< 10 \text{ ng m}^{-2} \text{ s}^{-1}$). Maximum HONO emissions were somewhat higher than maximum NO emissions, especially for bare soil. Integrating full wetting and drying cycles (6-8 hours), 0.04-1.9 mg m^{-2} HONO-N and 0.06-1.6 mg m^{-2} NO-N were released (Fig. 5, lower panel). While the maximum fluxes of reactive nitrogen emission were higher for HONO than NO, especially from bare soil, the integrated emissions were similar or even larger for NO, which is released over a wider range of SWC.

In general, it is difficult to compare chamber flux measurements of different studies due to different experimental configurations, such as chamber dimension, flow rate, resident time and drying rate etc. Here, we compared our results to studies which applied the same method (with the same or very similar conditions). The emission rates were consistent with these studies where HONO-N or NO-N emissions from soil between 1-3000 $\text{ng m}^{-2} \text{ s}^{-1}$ were found (Su et al., 2011; Oswald et al., 2013; Mamtimin et al., 2016; Wu et al., 2014; Weber et al., 2015). Mamtimin et al. (2016) observed NO-N fluxes at 25°C of 57.5 $\text{ng m}^{-2} \text{ s}^{-1}$, 18.9 $\text{ng m}^{-2} \text{ s}^{-1}$ and 4.1 $\text{ng m}^{-2} \text{ s}^{-1}$ for soil of grape and cotton fields and desert soil from an oasis in China, respectively. Oswald et al. (2013) found HONO-N and NO-N emissions between 2 and 280 $\text{ng m}^{-2} \text{ s}^{-1}$ (each) from different soil from all over the world covering a wide range of pH, nutrient content and organic matter. Biogenic NO emissions of 44 soil samples from arid and semi-arid regions were reviewed by Meixner and Yang (2006) with N-fluxes ranging from 0 to 142 $\text{ng m}^{-2} \text{ s}^{-1}$.

In contrast to the results of the present study, where bare soil showed highest emissions, Weber et al. (2015) found lowest emission from bare soil in samples from South Africa. In that study, dark cyanobacteria-dominated biocrusts revealed highest emission rates (each HONO-N and NO-N up to 200 ng m⁻² s⁻¹), followed by light cyanobacteria-dominated biocrusts (up to 120 ng m⁻² s⁻¹), whereas in the present study, emissions of dark cyanobacteria-dominated biocrusts tended to be lower. No significant difference of HONO-N and NO-N emissions from light BSC between both sample origins were found. HONO-N and NO-N emissions of moss- and chlorolichen-dominated biocrusts were low in both studies (each <60 ng m⁻² s⁻¹) but still significantly higher for samples from South Africa than from Cyprus. In the present study HONO maximum emissions were higher than for NO (while integrated emissions being comparable) while in the study of Weber et al. (2015) HONO maximum fluxes were somewhat lower than those of NO. The present results of nitrogen emissions correlated well with the nutrient contents (especially NO₂⁻ and NO₃⁻, Fig. 6). Bare soil, in which highest NO₃⁻ and NO₂⁻ levels were found, also showed highest HONO and NO emissions. A good linear correlation was found between NO₂⁻ contents and emission of both nitrogen gas phase species for all samples (R² = 0.84 for HONO and 0.85 for NO; p<0.001). The level of correlation between NO₃⁻ and HONO and NO was lower, but still significant (R² = 0.68 and 0.67, respectively, p<0.001). Low correlations were found between HONO or NO emissions and NH₄⁺-contents (R² = 0.165 and 0.232; p=0.05). Thus, in the present study it seems that reactive nitrogen emissions predominantly depend on NO₂⁻ and NO₃⁻ contents and not on surface cover types, although biocrusts (especially with cyanobacteria and cyanolichens) are able to fix atmospheric nitrogen (Belnap, 2002; Elbert et al., 2012; Barger et al., 2013; Patova et al., 2016). The results of a two-factorial ANOVA showed that HONO or NO emissions were not significantly related to soil cover type but rather with nitrite content, i.e., its direct aqueous precursor. For nitrate, the two-factorial ANOVA indicated dependencies of both cover type and nutrient content. **Nevertheless, a dominant contribution from microbial activity to the nutrient content is anticipated. Long range transport and atmospheric deposition of NO_x and nitrate/nitrite/ammonium can be excluded to be a dominant source of HONO and NO precursors in local soil, as the observed concentrations in Cyprus ambient air were very low (Meusel et al., 2016; Kleanthous et al., 2014). Furthermore it was not possible to determine the microbial community below the biocrust or in bare soil.** Although biocrusts increase nutrient availability via N fixation, it is their possible associations with ammonia oxidizing microbes (bacterial and archaea) that finally convert the fixed nitrogen to nitrite and nitrate. **Nitrification and other nitrogen cycling processes are not restricted to biocrusts, but can also occur in non-crusts soils. The relevance of these processes is expected to depend on substrate richness (i.e. amount of ammonium available for nitrifiers).** Our results differ from those obtained by Weber et al. (2015) on South African samples, as there HONO and NO emissions were not correlated with bulk concentrations of ammonium, nitrite and nitrate. In their study nitrite content was lowest for bare soil compared to other biocrust types. Ammonium and nitrite levels were also lower than in the present study. Therefore Weber et al. (2015) indicated that biocrusts can enhance N-cycle and emission of reactive nitrogen.

Since most of the samples were slightly alkaline and only moss samples were slightly acidic, no effect of pH could be observed. But in general it is expected that with higher nutrient and lower pH values HONO emission is increased by simple partitioning processes (Su et al., 2011). The simulated equilibrium concentration at soil surface [HONO]* (equation see Su et al., 2011) is much lower than the measured one. This deviation is probably based on the non-ideal

behavior of the soil samples (adsorption, Kelvin and solute interaction effects on gas/liquid partitioning). But this method does not allow argumentation on physical or biological processes.

3.4 Comparison of soil emission and observed missing source

To quantify the flux rate of HONO emissions from soil to the local atmosphere and to compare it to the unaccounted source found in Cyprus in 2014 (Meusel et al., 2016), we applied a standard formalism describing the atmosphere-soil exchange of trace gases as a function of the difference between the atmospheric concentration and the equilibrium concentration at the soil solution surface $[HONO]^*$ (Su et al., 2011):

$$F^* = v_T ([HONO]^* - [HONO]) \quad (\text{eq.5})$$

where $[HONO]$ is the ambient HONO concentration measured on Cyprus (mean daytime average 60 ppt) and $[HONO]^*$ is the equilibrium concentration at soil surface. $[HONO]^*$ can be determined from measurements in a static chamber. In a dynamic chamber system, there is a concentration gradient of HONO between the headspace (where HONO was measured) and the soil surface. Here we used the measurements of water vapor to correct for the soil surface concentration and equilibrium concentration of HONO by assuming a similar gradient for the two species. A correction coefficient of 3.8 was determined, which is the ratio of the equilibrium rH of 100% over wet soil surface to the initial headspace rH of 25-30% after inserting the wet sample into the chamber. The transfer velocity, v_t , depends primarily on meteorological and soil conditions, and is typically on the order of $\sim 1 \text{ cm s}^{-1}$. The flux rate of NO was calculated accordingly with mean daytime NO concentrations of 38 ppt. The calculated flux F^* was about $(67 \pm 3) \%$ of the flux measured in the chamber.

The distribution of nine different surface cover types was mapped (Fig. 2), including stones, vascular vegetation and litter not being attributed to emit significant amounts of HONO and NO to the atmosphere. The residual HONO emitting surface covers comprised 45.6% of total surface in the investigated area. Combining the information on soil/biocrust population and the calculated flux F^* , a site-specific community emission F_{comm} of HONO and NO can be estimated via following equation (eq. 6).

$$F_{\text{comm,max}} = \sum_i^{\text{type}} F_{\text{max},i}^* \cdot p_i / 100 \quad \text{or} \quad F_{\text{comm,int}} = \sum_i^{\text{type}} F_{\text{int},i}^* \cdot p_i / 100 \quad (\text{eq. 6})$$

where F_{comm} denotes the estimated community flux, $F_{\text{max},i}^*$ or $F_{\text{int},i}^*$ the maximum or integrated emission rates of each individual surface cover type i [$\text{ng N m}^{-2} \text{ s}^{-1}$ or $\mu\text{g N m}^{-2}$] and p_i the fraction of population type i [%].

Under optimum soil water conditions (20-30% WHC) and constant temperatures of about 25°C , between 2.2 and $18.8 \text{ ng m}^{-2} \text{ s}^{-1}$ of total HONO-N and 1.6 - $16.2 \text{ ng m}^{-2} \text{ s}^{-1}$ of total NO-N are emitted from the different crust/soil population combinations derived from the vegetation cover assessment. In the lower range of total emissions the contribution from bare soil dominates with up to 69% (HONO) and 55% (NO), respectively, followed by moss BSC (HONO: 23%; NO: 32%). At high levels of total emission, the contribution from light BSC dominates (HONO: 43%, NO: 49%), decreasing the contribution of bare soil down to about 25% (HONO) and 13% (NO). Emissions from dark BSC contribute about 20% or 24% to the total HONO or NO flux while the contribution from moss BSC decreases to 10% or 12%, respectively. Emissions from chlorolichen BSC don't play a significant role ($< 2.4\%$) in general (see Fig. 7).

After heavy rainfalls moistening the soil to full water-holding capacity, 11 - $113 \mu\text{g m}^{-2}$ of HONO-N and 10 - $131 \mu\text{g m}^{-2}$ of NO-N can be calculated for one complete wetting-and-drying period. Assuming 30 rain events per year (based

on the statistic of 4 years precipitation data), a wetting-drying cycle time of 7 days, and constant emissions in between them (at 10% WHC) up to $160 \text{ mg m}^{-2} \text{ yr}^{-1}$ of nitrogen can be emitted directly by the sum of HONO-N and NO-N from Cyprus natural ground surfaces, i.e., excluding heterogeneous conversion of NO_2 on ground surface.

The release of HONO from the ground surface to the atmosphere can be related to the atmospheric HONO production rate via eq. 7 (adapted from Su et al., 2011) and then compared to the missing source.

$$S_{\text{ground}} = \frac{F_{\text{commmax}}(T, \text{SWC})}{\text{BLH}} * a \quad (\text{eq.7})$$

with S_{ground} : HONO or NO emitted from ground surface; BLH: boundary layer height (mixed layer height) and a : factor to convert ng N in number of molecules ($10^{-9} * 6.022 \times 10^{23} / 14$).

During the CYPHEX campaign in summer 2014 a mean boundary layer height of 300 m above ground layer was observed by means of a ceilometer. Due to missing precipitation during CYPHEX, but high relative humidity prevailing (CYPHEX 2014: 75-100%), a mean soil water content of 10% WHC (at 25°C) can be estimated (Likos, 2008; Leelamanie, 2010), reducing the HONO source strength to 35% of the emission maximum at optimum SWC. Integrating the lowermost versus the uppermost observed HONO emissions per soil/crust type, the emissions at 25°C and a SWC of 10% WHC would span a wide range between 1.1×10^5 and $9.6 \times 10^5 \text{ cm}^{-3} \text{ s}^{-1}$, covering 9 to 73% of the missing mean source of $1.3 \times 10^6 \text{ cm}^{-3} \text{ s}^{-1}$ observed in the field (Meusel et al., 2016). However, temperatures in the field have strong diel cycles, and a temperature increase from 25°C to 50°C has been shown to lead to 6-10 times higher emission at constant SWC (Oswald et al., 2013; Mamtimin et al., 2016). On Cyprus the observed soil surface temperatures changed from 10°C during night up to 45°C during daytime (Fig. 8, red line, or Fig. S2). In the natural habitat the micrometeorological parameters change in concert, i.e., with increasing temperature the SWC decreases, influencing the flux-enhancing effect of temperature. Based on the assumption of a linear change of SWC with temperature a diel course of the SWC between 6 and 14% of WHC is simulated (Fig. 8, blue line), lowering the emission flux (22-49% of optimum). Applying the described SWC dependence and the temperature dependence on flux rates as reported by Oswald et al. (2013), high daytime temperatures increase the simulated diel course of HONO-N flux up to daytime maximum of $7.4 \text{ ng m}^{-2} \text{ s}^{-1}$ (Fig. 8, lower panel), but with a notable dip at high noon, due to the opposing effect of decreasing SWC at higher temperatures. The NO-N emissions show a similar pattern, with a slightly lower flux range (up to $6.4 \text{ ng m}^{-2} \text{ s}^{-1}$). Converted into production rates (eq. 7), the ground based soil and biocrust emissions at noon would be up to $1.1 \times 10^6 \text{ cm}^{-3} \text{ s}^{-1}$ HONO-N and $0.9 \times 10^6 \text{ cm}^{-3} \text{ s}^{-1}$ NO-N covering up to 85% and 8.5% of the missing HONO and NO source found during CYPHEX 2014 (Meusel et al., 2016). Note that during CYPHEX there were two periods with lower rH, in which even a NO sink was detected. In some mornings of the campaign dew formation was expected causing an increase in soil humidity. Combined with rising temperatures after sun-rise these optimized meteorological conditions may have led to enhanced soil emissions and would confer a reasonable explanation for the strong HONO morning peaks observed during the campaign.

Field observations (VandenBoer et al., 2013; Zhang et al., 2009; Tsai et al. 2017) as well as model results (Wong et al., 2013) showed that HONO concentrations typically decrease exponentially from the surface upwards. Eq. 7 does not include a chemistry-transport model, nor accounts for the existence of a vertical profile of concentrations, which may bias the calculation on HONO source strength. But the method for predicting the ground source using homogeneous mixed air columns is consistent with other recent studies (Stemmler et al., 2006; Tsai et al., 2017).

Tsai et al. (2017) clearly showed the presence of an important ground source of daytime HONO at a rural basin in Utah, during wintertime (no snow, low temperatures). They inferred that ground surface fluxes may account for 63±32% of the unidentified HONO daytime source throughout the day. HONO-N fluxes of up to 7.4 ng m⁻² s⁻¹ (Fig. 8, lower panel) determined in this study are comparable to HONO-N fluxes found in other regions, e.g., 2.7 ng m⁻² s⁻¹ reported for the northern Michigan forest canopy (Zhang et al., 2009; Zhou et al., 2011), the average daytime HONO-N flux of 7.0 ng m⁻² s⁻¹ measured over an agricultural field in Bakersfield (Ren et al., 2011), and the average HONO-N flux of about 11.6 ng m⁻² s⁻¹ measured by Tsai et al. (2017). In contrast to the present study, the latter concluded that, under the prevailing high NO_x conditions, the respective HONO formation was related to solar radiation and NO₂ mixing ratios, such as photo-enhanced conversion of NO₂ or nitrate photolysis on the ground. This can be ruled out in this study, as pure air (no NO₂) was used to purge the chambers and no light was applied. While in Cyprus the observed soil emissions can explain high amounts of atmospheric HONO, other studies excluded soil emission to be a dominant source (Oswald et al., 2015; Laufs et al., 2017). Oswald et al. (2015) studied soil samples from a boreal forest in Finland and observed HONO emission below the detection limit. But those samples had very low nutrient contents and were highly acidic (pH ≈ 3) for which microbial activity is supposed to be low (Fierer and Jackson, 2006; Persson and Wiren, 1995; Ste-Marie and Pare, 1999; Simek and Cooper, 2002). Similarly, Laufs et al. (2017) didn't find correlations between HONO fluxes and temperature or humidity measured in the field, and concluded that other HONO sources than biological soil emission must have been dominated. In contrast to the soil water content in Cyprus, the water contents at the field site studied by Laufs et al. (2016) were higher than the optimum soil water content presented by Oswald et al. (2013).

4 Conclusions

HONO and NO emission rates from soil and biological soil crusts were derived by means of lab-based enclosure trace gas exchange measurements, and revealed quite similar ranges of reactive nitrogen source strengths. Emissions of both compounds strongly correlated with NO₂⁻ and NO₃⁻ content of the samples. Emissions from bare soil were highest, but bare soil surface spots were rarely found at the investigated CYPHEX field study site. The estimated total ground surface HONO flux in the natural habitat was consistent with the previously unaccounted source estimated for Cyprus, i.e., the unaccounted HONO source can essentially be explained by emissions from soil/biocrusts. For NO, the measured and simulated fluxes cannot account for the unaccounted NO source (during the humid periods of the CYPHEX campaign 2014), indicating that emission from soil was not the only missing source of NO.

References

Abed, R. M. M., Lam, P., de Beer, D., and Stief, P.: High rates of denitrification and nitrous oxide emission in arid biological soil crusts from the Sultanate of Oman, *Isme Journal*, 7, 1862-1875, 10.1038/ismej.2013.55, 2013.

- 1 Aliche, B., Platt, U., and Stutz, J.: Impact of nitrous acid photolysis on the total hydroxyl radical budget during the
2 Limitation of Oxidant Production/Pianura Padana Produzione di Ozono study in Milan, Journal of Geophysical
3 Research-Atmospheres, 107, 10.1029/2000jd000075, 2002.
- 4 Ammann, M., Kalberer, M., Jost, D. T., Tobler, L., Rossler, E., Piguet, D., Gaggeler, H. W., and Baltensperger, U.:
5 Heterogeneous production of nitrous acid on soot in polluted air masses, Nature, 395, 157-160, 10.1038/25965,
6 1998.
- 7 Arens, F., Gutzwiller, L., Baltensperger, U., Gaggeler, H. W., and Ammann, M.: Heterogeneous reaction of NO₂ on
8 diesel soot particles, Environmental Science & Technology, 35, 2191-2199, 10.1021/es000207s, 2001.
- 9 Aubin, D. G., and Abbatt, J. P. D.: Interaction of NO₂ with hydrocarbon soot: Focus on HONO yield, surface
10 modification, and mechanism, Journal of Physical Chemistry A, 111, 6263-6273, 10.1021/jp068884h, 2007.
- 11 Baergen, A. M., and Donaldson, D. J.: Photochemical renoxification of nitric acid on real urban grime,
12 Environmental Science & Technology, 47, 815-820, 10.1021/es3037862, 2013.
- 13 Barger, N. N., Castle, S. C., and Dean, G. N.: Denitrification from nitrogen-fixing biologically crusted soils in a cool
14 desert environment, southeast Utah, USA, Ecological Processes, 2, 16, 10.1186/2192-1709-2-16, 2013.
- 15 Barger, N. N., Weber, B., Garcia-Pichel, F., Zaady, E., Belnap, J.: Patterns and controls on nitrogen cycling of
16 biological soil crusts. In: Weber, B., Büdel, B., Belnap, J. (eds) Biological soil crusts: An organizing principle in
17 drylands, Ecological Studies 226, Springer International Publishing Switzerland, pp 257-285, 2016.
- 18 Bejan, I., Abd El Aal, Y., Barnes, I., Benter, T., Bohn, B., Wiesen, P., and Kleffmann, J.: The photolysis of ortho-
19 nitrophenols: a new gas phase source of HONO, Physical Chemistry Chemical Physics, 8, 2028-2035,
20 10.1039/b516590c, 2006.
- 21 Belnap, J.: Nitrogen fixation in biological soil crusts from southeast Utah, USA, Biology and Fertility of Soils, 35,
22 128-135, 10.1007/s00374-002-0452-x, 2002.
- 23 Belnap, J., Weber, B., Büdel, B.: Biological soil crusts as an organizing principle in drylands. In: Weber, B., Büdel,
24 B., Belnap, J. (eds) Biological soil crusts: An organizing principle in drylands, Ecological Studies 226, Springer
25 International Publishing Switzerland, pp 3-13, 2016.
- 26 Broske, R., Kleffmann, J., and Wiesen, P.: Heterogeneous conversion of NO₂ on secondary organic aerosol surfaces:
27 A possible source of nitrous acid (HONO) in the atmosphere?, Atmospheric Chemistry and Physics, 3, 469-474,
28 2003.
- 29 Büdel, B., Darienko, T., Deutschewitz, K., Dojani, S., Friedl, T., Mohr, K., Salisch, M., Reisser, W. and Weber, B.:
30 Southern African biological soil crusts are ubiquitous and highly diverse in drylands, being restricted by rainfall
31 frequency. Microbial Ecology 57(2): 229-47, 2009.
- 32 Cleveland, C. C., Townsend, A. R., Schimel, D. S., Fisher, H., Howarth, R. W., Hedin, L. O., Perakis, S. S., Latty, E.
33 F., Von Fischer, J. C., Elseroad, A., and Wasson, M. F.: Global patterns of terrestrial biological nitrogen (N₂)
34 fixation in natural ecosystems, Global Biogeochemical Cycles, 13, 623-645, 10.1029/1999gb900014, 1999.
- 35 Czader, B. H., Rappenglueck, B., Percell, P., Byun, D. W., Ngan, F., and Kim, S.: Modeling nitrous acid and its
36 impact on ozone and hydroxyl radical during the Texas Air Quality Study 2006, Atmospheric Chemistry and
37 Physics, 12, 6939-6951, 10.5194/acp-12-6939-2012, 2012.

- 1 Darby, B. J., Neher, D. A.: Microfauna within biological soil crusts. In: Weber, B., Büdel, B., Belnap, J. (eds)
- 2 Biological soil crusts: An organizing principle in drylands, Ecological Studies 226, Springer International
- 3 Publishing Switzerland, pp 139-157, 2016.
- 4 Dumack, K., Koller, R., Weber, B. and Bonkowski, M.: Estimated heterotrophic protist abundances and their
- 5 diversity in South African biological soil crusts. South African Journal of Science 112(7/8). Art. #2015-0302, 5
- 6 pages. <http://dx.doi.org/10.17159/sajs.2016/20150302>, 2016
- 7 Elbert, W., Weber, B., Burrows, S., Steinkamp, J., Budel, B., Andreae, M. O., and Poschl, U.: Contribution of
- 8 cryptogamic covers to the global cycles of carbon and nitrogen, Nature Geosci, 5, 459-462,
- 9 <http://www.nature.com/ngeo/journal/v5/n7/abs/ngeo1486.html#supplementary-information>, 2012.
- 10 Fierer, N., and Jackson, R. B.: The diversity and biogeography of soil bacterial communities, Proceedings of the
- 11 National Academy of Sciences of the United States of America, 103, 626-631, 10.1073/pnas.0507535103, 2006.
- 12 George, C., Streckowski, R. S., Kleffmann, J., Stemmler, K., and Ammann, M.: Photoenhanced uptake of gaseous
- 13 NO₂ on solid-organic compounds: a photochemical source of HONO?, Faraday Discussions, 130, 195-210,
- 14 10.1039/b417888m, 2005.
- 15 Han, C., Yang, W. J., Wu, Q. Q., Yang, H., and Xue, X. X.: Heterogeneous photochemical conversion of NO₂ to
- 16 HONO on the humic acid surface under simulated sunlight, Environmental Science & Technology, 50, 5017-
- 17 5023, 10.1021/acs.est.5b05101, 2016.
- 18 Harrison, R. M., and Kitto, A. M. N.: Evidence for a surface source of atmospheric nitrous acid, Atmospheric
- 19 Environment, 28, 1089-1094, 10.1016/1352-2310(94)90286-0, 1994.
- 20 Herridge, D. F., Peoples, M. B., and Boddey, R. M.: Global inputs of biological nitrogen fixation in agricultural
- 21 systems, Plant and Soil, 311, 1-18, 10.1007/s11104-008-9668-3, 2008.
- 22 Johnson, S. L., Budinoff, C. R., Belnap, J., and Garcia-Pichel, F.: Relevance of ammonium oxidation within
- 23 biological soil crust communities, Environmental Microbiology, 7, 1-12, 10.1111/j.1462-2920.2004.00649.x,
- 24 2005.
- 25 Kalberer, M., Ammann, M., Arens, F., Gaggeler, H. W., and Baltensperger, U.: Heterogeneous formation of nitrous
- 26 acid (HONO) on soot aerosol particles, Journal of Geophysical Research-Atmospheres, 104, 13825-13832,
- 27 10.1029/1999jd900141, 1999.
- 28 Kebede, M. A., Scharko, N. K., Appelt, L. E., and Raff, J. D.: Formation of nitrous acid during ammonia
- 29 photooxidation on TiO₂ under atmospherically relevant conditions, Journal of Physical Chemistry Letters, 4,
- 30 2618-2623, 10.1021/jz401250k, 2013.
- 31 Kinugawa, T., Enami, S., Yabushita, A., Kawasaki, M., Hoffmann, M. R., and Colussi, A. J.: Conversion of gaseous
- 32 nitrogen dioxide to nitrate and nitrite on aqueous surfactants, Physical Chemistry Chemical Physics, 13, 5144-
- 33 5149, 10.1039/C0CP01497D, 2011.
- 34 Kleanthous, S., Vrekoussis, M., Mihalopoulos, N., Kalabokas, P., and Lelieveld, J.: On the temporal and spatial
- 35 variation of ozone in Cyprus, Science of The Total Environment, 476-477, 677-687,
- 36 <http://dx.doi.org/10.1016/j.scitotenv.2013.12.101>, 2014.
- 37 Kleffmann, J., H. Becker, K., Lackhoff, M., and Wiesen, P.: Heterogeneous conversion of NO₂ on carbonaceous
- 38 surfaces, Physical Chemistry Chemical Physics, 1, 5443-5450, 10.1039/A905545B, 1999.

- 1 Kleffmann, J., Kurtenbach, R., Lorzer, J., Wiesen, P., Kalthoff, N., Vogel, B., and Vogel, H.: Measured and
2 simulated vertical profiles of nitrous acid - Part I: Field measurements, *Atmospheric Environment*, 37, 2949-
3 2955, 10.1016/s1352-2310(03)00242-5, 2003.
- 4 Kleffmann, J., Gavriloaiei, T., Hofzumahaus, A., Holland, F., Koppmann, R., Rupp, L., Schlosser, E., Siese, M., and
5 Wahner, A.: Daytime formation of nitrous acid: A major source of OH radicals in a forest, *Geophysical Research*
6 *Letters*, 32, 10.1029/2005gl022524, 2005.
- 7 Kleffmann, J., and Wiesen, P.: Heterogeneous conversion of NO₂ and NO on HNO₃ treated soot surfaces:
8 atmospheric implications, *Atmospheric Chemistry and Physics*, 5, 77-83, 2005.
- 9 Langridge, J. M., Gustafsson, R. J., Griffiths, P. T., Cox, R. A., Lambert, R. M., and Jones, R. L.: Solar driven
10 nitrous acid formation on building material surfaces containing titanium dioxide: A concern for air quality in
11 urban areas?, *Atmospheric Environment*, 43, 5128-5131, <http://dx.doi.org/10.1016/j.atmosenv.2009.06.046>,
12 2009.
- 13 Laufs, S., Cazaunau, M., Stella, P., Kurtenbach, R., Cellier, P., Mellouki, A., Loubet, B., and Kleffmann, J.: Diurnal
14 fluxes of HONO above a crop rotation, *Atmos. Chem. Phys.*, 17, 6907-6923, 10.5194/acp-17-6907-2017, 2017.
- 15 Leelamanie, D. A. L.: Changes in Soil Water Content with Ambient Relative Humidity in Relation to the Organic
16 Matter and Clay. , *Tropical Agricultural Research and Extension*, 13, 6-10, 10.4038/tare.v13i1.3130, 2010.
- 17 Lelièvre, S., Bedjanian, Y., Laverdet, G., and Le Bras, G.: Heterogeneous reaction of NO₂ with hydrocarbon flame
18 soot, *The Journal of Physical Chemistry A*, 108, 10807-10817, 10.1021/jp0469970, 2004.
- 19 Li, X., Rohrer, F., Hofzumahaus, A., Brauers, T., Häseler, R., Bohn, B., Broch, S., Fuchs, H., Gomm, S., Holland, F.,
20 Jäger, J., Kaiser, J., Keutsch, F. N., Lohse, I., Lu, K., Tillmann, R., Wegener, R., Wolfe, G. M., Mentel, T. F.,
21 Kiendler-Scharr, A., and Wahner, A.: Missing gas-phase source of HONO inferred from Zeppelin measurements
22 in the troposphere, *Science*, 344, 292-296, 10.1126/science.1248999, 2014.
- 23 Likos, W. J.: Vapor adsorption index for expansive soil classification, *Journal of Geotechnical and*
24 *Geoenvironmental Engineering*, 134, 1005-1009, 10.1061/(asce)1090-0241(2008)134:7(1005), 2008.
- 25 Liu, Y., Han, C., Ma, J., Bao, X., and He, H.: Influence of relative humidity on heterogeneous kinetics of NO₂ on
26 kaolin and hematite, *Physical Chemistry Chemical Physics*, 17, 19424-19431, 10.1039/c5cp02223a, 2015.
- 27 Mamtimin, B., Meixner, F. X., Behrendt, T., Badawy, M., and Wagner, T.: The contribution of soil biogenic NO and
28 HONO emissions from a managed hyperarid ecosystem to the regional NO_x emissions during growing season,
29 *Atmos. Chem. Phys.*, 16, 10175-10194, 10.5194/acp-16-10175-2016, 2016.
- 30 Meixner, F. X., and Yang, W. X.: Biogenic emissions of nitric oxide and nitrous oxide from arid and semi-arid land,
31 in: *Dryland Ecohydrology*, edited by: D'Odorico, P., and Porporato, A., Springer Netherlands, Dordrecht, 233-
32 255, 2006.
- 33 Meusel, H., Kuhn, U., Reiffs, A., Mallik, C., Harder, H., Martinez, M., Schuladen, J., Bohn, B., Parchatka, U.,
34 Crowley, J. N., Fischer, H., Tomsche, L., Novelli, A., Hoffmann, T., Janssen, R. H. H., Hartogensis, O., Pikridas,
35 M., Vrekoussis, M., Bourtsoukidis, E., Weber, B., Lelieveld, J., Williams, J., Pöschl, U., Cheng, Y., and Su, H.:
36 Daytime formation of nitrous acid at a coastal remote site in Cyprus indicating a common ground source of
37 atmospheric HONO and NO, *Atmos. Chem. Phys.*, 16, 14475-14493, 10.5194/acp-16-14475-2016, 2016.

- 1 Meusel, H., Elshorbany, Y., Kuhn, U., Bartels-Rausch, T., Reinmuth-Selzle, K., Kampf, C. J., Li, G., Wang, X.,
2 Lelieveld, J., Pöschl, U., Hoffmann, T., Su, H., Ammann, M., and Cheng, Y.: Light-induced protein nitration and
3 degradation with HONO emission, *Atmos. Chem. Phys. Discuss.*, 2017, 1-22, 10.5194/acp-2017-277, 2017.
- 4 Michoud, V., Colomb, A., Borbon, A., Miet, K., Beekmann, M., Camredon, M., Aumont, B., Perrier, S., Zapf, P.,
5 Siour, G., Ait-Helal, W., Afif, C., Kukui, A., Furger, M., Dupont, J. C., Haeffelin, M., and Doussin, J. F.: Study
6 of the unknown HONO daytime source at a European suburban site during the MEGAPOLI summer and winter
7 field campaigns, *Atmospheric Chemistry and Physics*, 14, 2805-2822, 10.5194/acp-14-2805-2014, 2014.
- 8 Monge, M. E., D'Anna, B., Mazri, L., Giroir-Fendler, A., Ammann, M., Donaldson, D. J., and George, C.: Light
9 changes the atmospheric reactivity of soot, *Proceedings of the National Academy of Sciences of the United States*
10 *of America*, 107, 6605-6609, 10.1073/pnas.0908341107, 2010.
- 11 Ndour, M., D'Anna, B., George, C., Ka, O., Balkanski, Y., Kleffmann, J., Stemmler, K., and Ammann, M.:
12 Photoenhanced uptake of NO₂ on mineral dust: Laboratory experiments and model simulations, *Geophysical*
13 *Research Letters*, 35, 10.1029/2007gl032006, 2008.
- 14 Neuman, J. A., Trainer, M., Brown, S. S., Min, K. E., Nowak, J. B., Parrish, D. D., Peischl, J., Pollack, I. B., Roberts,
15 J. M., Ryerson, T. B., and Veres, P. R.: HONO emission and production determined from airborne measurements
16 over the Southeast U.S, *Journal of Geophysical Research: Atmospheres*, 121, 9237-9250,
17 10.1002/2016JD025197, 2016.
- 18 Oswald, R., Behrendt, T., Ermel, M., Wu, D., Su, H., Cheng, Y., Breuninger, C., Moravek, A., Mouglin, E., Delon,
19 C., Loubet, B., Pommerening-Roeser, A., Soergel, M., Poeschl, U., Hoffmann, T., Andreae, M. O., Meixner, F.
20 X., and Trebs, I.: HONO emissions from soil bacteria as a major source of atmospheric reactive nitrogen,
21 *Science*, 341, 1233-1235, 10.1126/science.1242266, 2013.
- 22 Oswald, R., Ermel, M., Hens, K., Novelli, A., Ouwersloot, H. G., Paasonen, P., Petaja, T., Sipila, M., Keronen, P.,
23 Back, J., Konigstedt, R., Beygi, Z. H., Fischer, H., Bohn, B., Kubistin, D., Harder, H., Martinez, M., Williams, J.,
24 Hoffmann, T., Trebs, I., and Soergel, M.: A comparison of HONO budgets for two measurement heights at a field
25 station within the boreal forest in Finland, *Atmospheric Chemistry and Physics*, 15, 799-813, 10.5194/acp-15-
26 799-2015, 2015.
- 27 Patova, E., Sivkov, M., and Patova, A.: Nitrogen fixation activity in biological soil crusts dominated by
28 cyanobacteria in the Subpolar Urals (European North-East Russia), *FEMS Microbiology Ecology*, 92,
29 10.1093/femsec/fiw131, 2016.
- 30 Persson, T., and Wirén, A.: Nitrogen mineralization and potential nitrification at different depths in acid forest soils,
31 *Plant and Soil*, 168, 55-65, 10.1007/bf00029313, 1995.
- 32 Pilegaard, K.: Processes regulating nitric oxide emissions from soils, *Philosophical Transactions of the Royal Society*
33 *B: Biological Sciences*, 368, 10.1098/rstb.2013.0126, 2013.
- 34 Ramazan, K. A., Syomin, D., and Finlayson-Pitts, B. J.: The photochemical production of HONO during the
35 heterogeneous hydrolysis of NO₂, *Physical Chemistry Chemical Physics*, 6, 3836-3843, 10.1039/b402195a, 2004.
- 36 Ren, X. R., Harder, H., Martinez, M., Leshner, R. L., Oliger, A., Simpas, J. B., Brune, W. H., Schwab, J. J.,
37 Demerjian, K. L., He, Y., Zhou, X. L., and Gao, H. G.: OH and HO₂ chemistry in the urban atmosphere of New
38 York City, *Atmospheric Environment*, 37, 3639-3651, 10.1016/s1352-2310(03)00459-x, 2003.

- 1 Ren, X., Brune, W. H., Oliger, A., Metcalf, A. R., Simpas, J. B., Shirley, T., Schwab, J. J., Bai, C., Roychowdhury,
2 U., Li, Y., Cai, C., Demerjian, K. L., He, Y., Zhou, X., Gao, H., and Hou, J.: OH, HO₂, and OH reactivity during
3 the PMTACS-NY Whiteface Mountain 2002 campaign: Observations and model comparison, *Journal of*
4 *Geophysical Research-Atmospheres*, 111, 10.1029/2005jd006126, 2006.
- 5 Ren, X., Sanders, J. E., Rajendran, A., Weber, R. J., Goldstein, A. H., Pusede, S. E., Browne, E. C., Min, K. E., and
6 Cohen, R. C.: A relaxed eddy accumulation system for measuring vertical fluxes of nitrous acid, *Atmospheric*
7 *Measurement Techniques*, 4, 2093-2103, 10.5194/amt-4-2093-2011, 2011.
- 8 Ronen, R., and Galun, M.: Pigment extraction from lichens with dimethylsulfoxide (DMSO) and estimation of
9 chlorophyll degradation, *Environmental and Experimental Botany*, 24, 239-245, 10.1016/0098-8472(84)90004-2,
10 1984.
- 11 Rummel, U., Ammann, C., Gut, A., Meixner, F. X., and Andreae, M. O.: Eddy covariance measurements of nitric
12 oxide flux within an Amazonian rain forest, *Journal of Geophysical Research: Atmospheres*, 107, LBA 17-11-
13 LBA 17-19, 10.1029/2001JD000520, 2002.
- 14 Sarwar, G., Roselle, S. J., Mathur, R., Appel, W., Dennis, R. L., and Vogel, B.: A comparison of CMAQ HONO
15 predictions with observations from the Northeast Oxidant and Particle Study, *Atmospheric Environment*, 42,
16 5760-5770, <http://dx.doi.org/10.1016/j.atmosenv.2007.12.065>, 2008.
- 17 Scharko, N. K., Berke, A. E., and Raff, J. D.: Release of nitrous acid and nitrogen dioxide from nitrate photolysis in
18 acidic aqueous solutions, *Environmental Science & Technology*, 48, 11991-12001, 10.1021/es503088x, 2014.
- 19 Šimek, M., and Cooper, J. E.: The influence of soil pH on denitrification: progress towards the understanding of this
20 interaction over the last 50 years, *European Journal of Soil Science*, 53, 345-354, 10.1046/j.1365-
21 2389.2002.00461.x, 2002.
- 22 Soergel, M., Regelin, E., Bozem, H., Diesch, J. M., Drewnick, F., Fischer, H., Harder, H., Held, A., Hosaynali-
23 Beygi, Z., Martinez, M., and Zetzsch, C.: Quantification of the unknown HONO daytime source and its relation
24 to NO₂, *Atmospheric Chemistry and Physics*, 11, 10433-10447, 10.5194/acp-11-10433-2011, 2011a.
- 25 Ste-Marie, C., and Paré, D.: Soil, pH and N availability effects on net nitrification in the forest floors of a range of
26 boreal forest stands, *Soil Biology and Biochemistry*, 31, 1579-1589, [http://dx.doi.org/10.1016/S0038-](http://dx.doi.org/10.1016/S0038-0717(99)00086-3)
27 [0717\(99\)00086-3](http://dx.doi.org/10.1016/S0038-0717(99)00086-3), 1999.
- 28 Stemmler, K., Ammann, M., Donders, C., Kleffmann, J., and George, C.: Photosensitized reduction of nitrogen
29 dioxide on humic acid as a source of nitrous acid, *Nature*, 440, 195-198, 10.1038/nature04603, 2006.
- 30 Stemmler, K., Ndour, M., Elshorbany, Y., Kleffmann, J., D'Anna, B., George, C., Bohn, B., and Ammann, M.: Light
31 induced conversion of nitrogen dioxide into nitrous acid on submicron humic acid aerosol, *Atmospheric*
32 *Chemistry and Physics*, 7, 4237-4248, 2007.
- 33 Strauss, S. L., Day, T. A., and Garcia-Pichel, F.: Nitrogen cycling in desert biological soil crusts across
34 biogeographic regions in the Southwestern United States, *Biogeochemistry*, 108, 171-182, 10.1007/s10533-011-
35 9587-x, 2012.
- 36 Stutz, J., Alicke, B., and Neftel, A.: Nitrous acid formation in the urban atmosphere: Gradient measurements of NO₂
37 and HONO over grass in Milan, Italy, *Journal of Geophysical Research-Atmospheres*, 107,
38 10.1029/2001jd000390, 2002.

- 1 Su, H., Cheng, Y. F., Cheng, P., Zhang, Y. H., Dong, S., Zeng, L. M., Wang, X., Slanina, J., Shao, M., and
2 Wiedensohler, A.: Observation of nighttime nitrous acid (HONO) formation at a non-urban site during PRIDE-
3 PRD2004 in China, *Atmospheric Environment*, 42, 6219-6232, 10.1016/j.atmosenv.2008.04.006, 2008a.
- 4 Su, H., Cheng, Y. F., Shao, M., Gao, D. F., Yu, Z. Y., Zeng, L. M., Slanina, J., Zhang, Y. H., and Wiedensohler, A.:
5 Nitrous acid (HONO) and its daytime sources at a rural site during the 2004 PRIDE-PRD experiment in China,
6 *Journal of Geophysical Research-Atmospheres*, 113, 10.1029/2007jd009060, 2008b.
- 7 Su, H., Cheng, Y., Oswald, R., Behrendt, T., Trebs, I., Meixner, F. X., Andreae, M. O., Cheng, P., Zhang, Y., and
8 Poeschl, U.: Soil nitrite as a source of atmospheric HONO and OH radicals, *Science*, 333, 1616-1618,
9 10.1126/science.1207687, 2011.
- 10 Tang, Y., An, J., Wang, F., Li, Y., Qu, Y., Chen, Y., and Lin, J.: Impacts of an unknown daytime HONO source on
11 the mixing ratio and budget of HONO, and hydroxyl, hydroperoxyl, and organic peroxy radicals, in the coastal
12 regions of China, *Atmospheric Chemistry and Physics*, 15, 9381-9398, 10.5194/acp-15-9381-2015, 2015.
- 13 Tsai, C., Spolaor, M., Colosimo, S. F., Pikelnaya, O., Cheung, R., Williams, E., Gilman, J. B., Lerner, B. M.,
14 Zamora, R. J., Warneke, C., Roberts, J. M., Ahmadov, R., de Gouw, J., Bates, T., Quinn, P. K., and Stutz, J.:
15 Nitrous acid formation in a snow-free wintertime polluted rural area, *Atmos. Chem. Phys. Discuss.*, 2017, 1-37,
16 10.5194/acp-2017-648, 2017.
- 17 VandenBoer, T. C., Brown, S. S., Murphy, J. G., Keene, W. C., Young, C. J., Pszenny, A. A. P., Kim, S., Warneke,
18 C., de Gouw, J. A., Maben, J. R., Wagner, N. L., Riedel, T. P., Thornton, J. A., Wolfe, D. E., Dubé, W. P.,
19 Öztürk, F., Brock, C. A., Grossberg, N., Lefer, B., Lerner, B., Middlebrook, A. M., and Roberts, J. M.:
20 Understanding the role of the ground surface in HONO vertical structure: High resolution vertical profiles during
21 NACHTT-11, *Journal of Geophysical Research: Atmospheres*, 118, 10.1029/2013JD020211, 10.1002/jgrd.50721, 2013.
- 22 van Dijk, S. M., Gut, A., Kirkman, G. A., Gomes, B. M., Meixner, F. X., and Andreae, M. O.: Biogenic NO
23 emissions from forest and pasture soils: Relating laboratory studies to field measurements, *Journal of*
24 *Geophysical Research: Atmospheres*, 107, LBA 25-21-LBA 25-11, 10.1029/2001JD000358, 2002.
- 25 Villena, G., Kleffmann, J., Kurtenbach, R., Wiesen, P., Lissi, E., Rubio, M. A., Croxatto, G., and Rappenglueck, B.:
26 Vertical gradients of HONO, NO_x and O₃ in Santiago de Chile, *Atmospheric Environment*, 45, 3867-3873,
27 10.1016/j.atmosenv.2011.01.073, 2011.
- 28 Vogel, B., Vogel, H., Kleffmann, J., and Kurtenbach, R.: Measured and simulated vertical profiles of nitrous acid -
29 Part II. Model simulations and indications for a photolytic source, *Atmospheric Environment*, 37, 2957-2966,
30 10.1016/s1352-2310(03)00243-7, 2003.
- 31 Wang, S. H., Ackermann, R., Spicer, C. W., Fast, J. D., Schmeling, M., and Stutz, J.: Atmospheric observations of
32 enhanced NO₂-HONO conversion on mineral dust particles, *Geophysical Research Letters*, 30,
33 10.1029/2003gl017014, 2003.
- 34 Weber, B., Wessels, D. C., Deutschewitz, K., Dojani, S., Reichenberger, H., and Büdel, B.: Ecological
35 characterization of soil-inhabiting and hypolithic soil crusts within the Knersvlakte, South Africa, *Ecological*
36 *Processes*, 2, 8, 10.1186/2192-1709-2-8, 2013.
- 37 Weber, B., Wu, D., Tamm, A., Ruckteschler, N., Rodriguez-Caballero, E., Steinkamp, J., Meusel, H., Elbert, W.,
38 Behrendt, T., Soergel, M., Cheng, Y., Crutzen, P. J., Su, H., and Poeschi, U.: Biological soil crusts accelerate the

nitrogen cycle through large NO and HONO emissions in drylands, *Proceedings of the National Academy of Sciences of the United States of America*, 112, 15384-15389, 10.1073/pnas.1515818112, 2015.

Wong, K. W., Tsai, C., Lefer, B., Haman, C., Grossberg, N., Brune, W. H., Ren, X., Luke, W., and Stutz, J.: Daytime HONO vertical gradients during SHARP 2009 in Houston, TX, *Atmospheric Chemistry and Physics*, 12, 635-652, 10.5194/acp-12-635-2012, 2012.

Wong, K. W., Tsai, C., Lefer, B., Grossberg, N., and Stutz, J.: Modeling of daytime HONO vertical gradients during SHARP 2009, *Atmospheric Chemistry and Physics*, 13, 3587-3601, 10.5194/acp-13-3587-2013, 2013.

Wu, D., Kampf, C. J., Pöschl, U., Oswald, R., Cui, J., Ermel, M., Hu, C., Trebs, I., and Sörgel, M.: Novel tracer method to measure isotopic labeled gas-phase nitrous acid (HO^{15}NO) in Biogeochemical Studies, *Environmental Science & Technology*, 48, 8021-8027, 10.1021/es501353x, 2014.

Yabushita, A., Enami, S., Sakamoto, Y., Kawasaki, M., Hoffmann, M. R., and Colussi, A. J.: Anion-catalyzed dissolution of NO_2 on aqueous microdroplets, *The Journal of Physical Chemistry A*, 113, 4844-4848, 10.1021/jp900685f, 2009.

Young, C. J., Washenfelder, R. A., Roberts, J. M., Mielke, L. H., Osthoff, H. D., Tsai, C., Pikel'naya, O., Stutz, J., Veres, P. R., Cochran, A. K., VandenBoer, T. C., Flynn, J., Grossberg, N., Haman, C. L., Lefer, B., Stark, H., Graus, M., de Gouw, J., Gilman, J. B., Kuster, W. C., and Brown, S. S.: Vertically resolved measurements of nighttime radical reservoirs; in Los Angeles and their contribution to the urban radical budget, *Environmental Science & Technology*, 46, 10965-10973, 10.1021/es302206a, 2012.

Zhang, N., Zhou, X. L., Shepson, P. B., Gao, H. L., Alaghmand, M., and Stirm, B.: Aircraft measurement of HONO vertical profiles over a forested region, *Geophysical Research Letters*, 36, 10.1029/2009gl038999, 2009.

Zhang, L., Wang, T., Zhang, Q., Zheng, J., Xu, Z., and Lv, M.: Potential sources of nitrous acid (HONO) and their impacts on ozone: A WRF-Chem study in a polluted subtropical region, *Journal of Geophysical Research: Atmospheres*, 121, 3645-3662, 10.1002/2015JD024468, 2016.

Zhou, X. L., Gao, H. L., He, Y., Huang, G., Bertman, S. B., Civerolo, K., and Schwab, J.: Nitric acid photolysis on surfaces in low- NO_x environments: Significant atmospheric implications, *Geophysical Research Letters*, 30, 10.1029/2003gl018620, 2003.

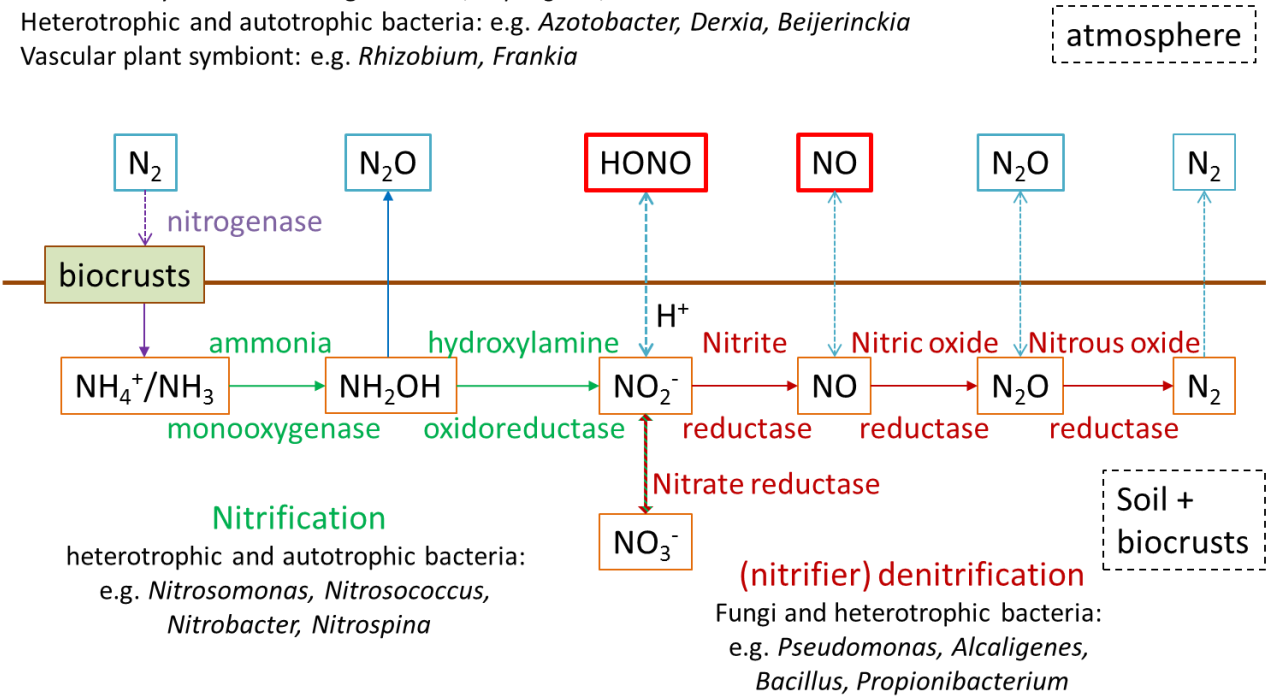
Zhou, X., Zhang, N., TerAvest, M., Tang, D., Hou, J., Bertman, S., Alaghmand, M., Shepson, P. B., Carroll, M. A., Griffith, S., Dusanter, S., and Stevens, P. S.: Nitric acid photolysis on forest canopy surface as a source for tropospheric nitrous acid, *Nature Geoscience*, 4, 440-443, 10.1038/ngeo1164, 2011.

1 **Table 1: Overview on the samples, distribution of replicates of soil/biocrust type and the different analysis:**

Type	Only nutrient analysis	Flux measurements, followed by nutrient and chlorophyll analysis	Sum
Bare soil	3	3	6
Dark BSC	3	5	8
Light BSC	3	4	10
Light BSC + cyanolichen	3		
Chlorolichen BSC I	3	3	12
Chlorolichen BSC II		6	
Moss BSC	3	4	7
Sum	18	25	43

2 **N₂ fixation**

3 Free living cyanobacteria: e.g. *Nostoc*, *Scytonema*, *Spirirestis*
 4 Lichenized cyanobacteria: e.g. *Collema*, *Leptogium*, *Lichinella*
 Heterotrophic and autotrophic bacteria: e.g. *Azotobacter*, *Derxia*, *Beijerinckia*
 Vascular plant symbiont: e.g. *Rhizobium*, *Frankia*



5 **Fig. 1: Nitrogen cycle at the atmosphere and pedosphere/biosphere interface including nitrogen fixation, nitrification,**
 6 **denitrification and emission. Involved enzymes and organisms are specified.**
 7

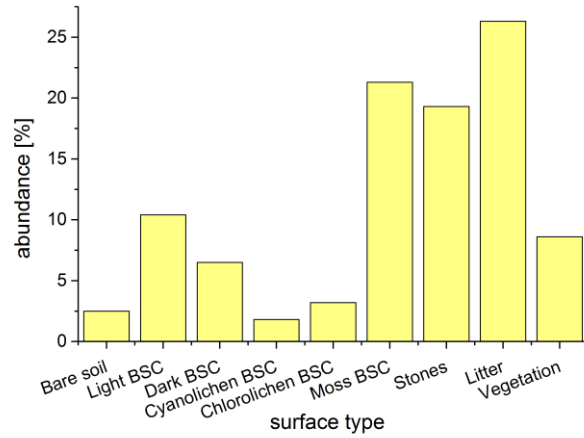


Fig. 2: Distribution of different types of ground surfaces in the studied area. Information derived from 50 grids.

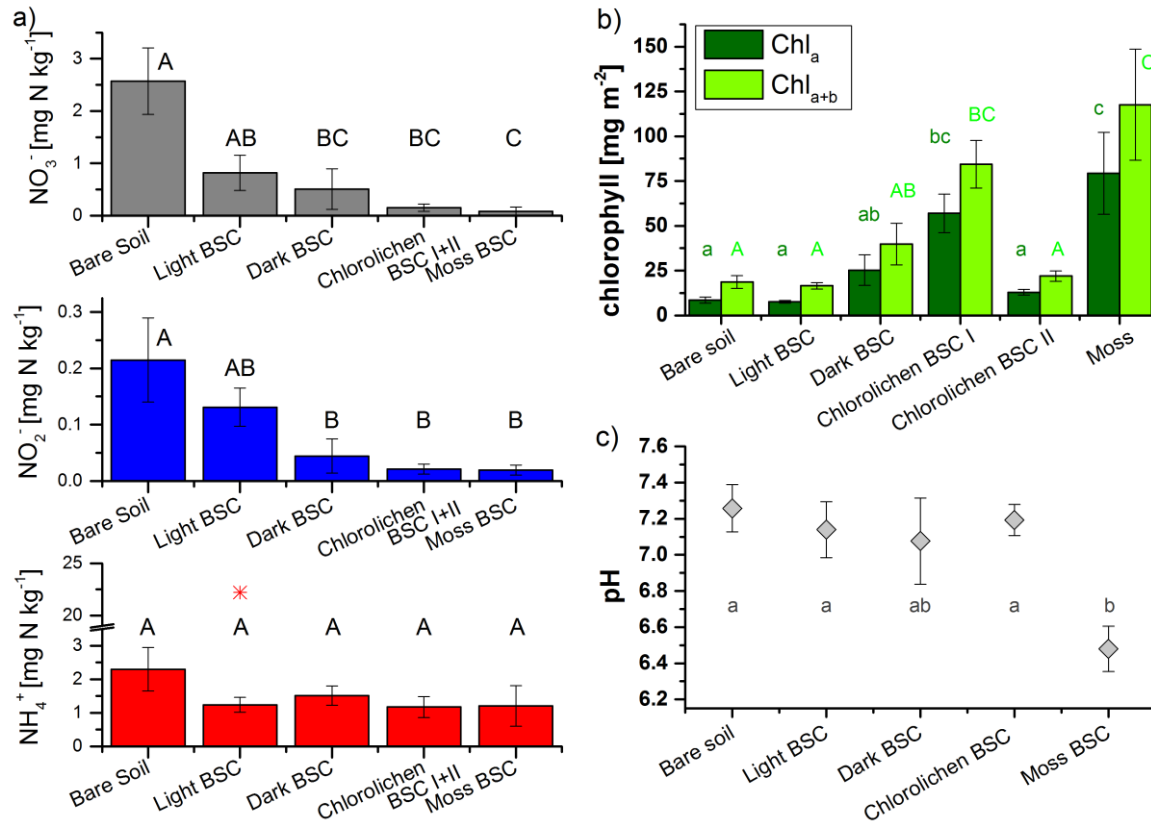


Fig. 3: Nutrient- and chlorophyll contents as well as pH values of bare soil and biocrust samples of different types. a) Nitrate, nitrite and ammonium content of all replicates. The red star indicates an outlier, b) chlorophyll a and chlorophyll a+b contents of samples after flux measurements c) pH values of samples without and after flux measurements (bare soil and moss BSC: n = 4; light, dark and chlorolichen BSC: n = 3). Number of replicates for a and b see table 1. In all 3 plots error bars indicate standard error of the mean and different letters indicate significant differences (of log-transformed data; p=0.05).

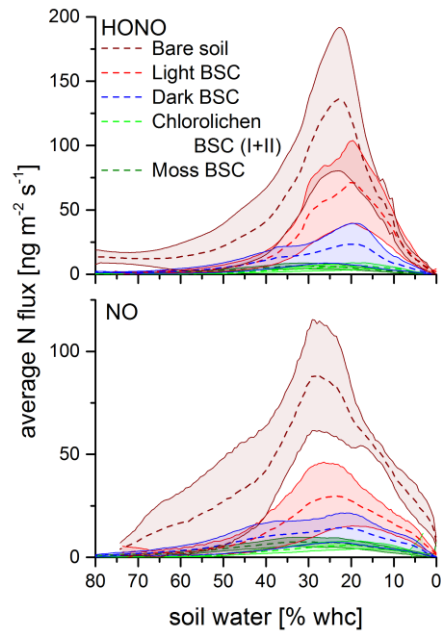


Fig. 4: HONO and NO emission fluxes as a function of soil water content. Dotted lines are the mean fluxes. Shaded areas indicate the standard deviation.

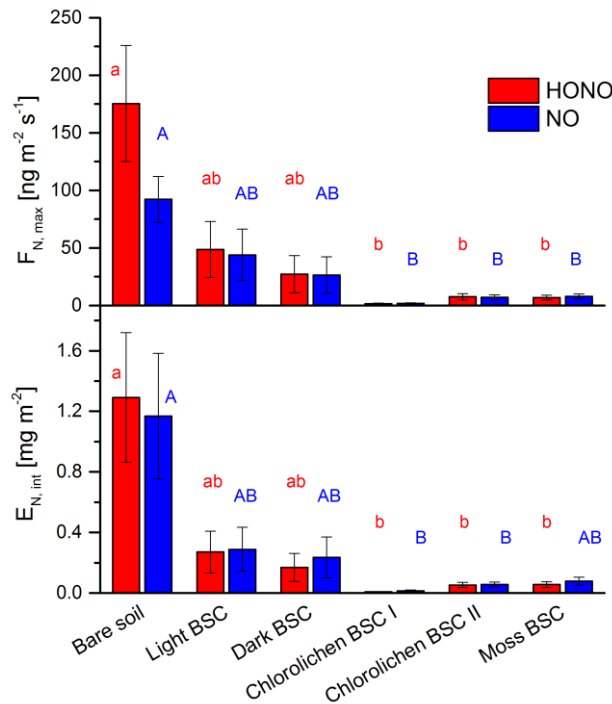


Fig. 5: Emission of HONO and NO from bare soil and biocrusts. Upper panel: Maximum HONO-N and NO-N fluxes in $\text{ng m}^{-2} \text{s}^{-1}$ at optimum water conditions; Lower panel: Emissions integrated over a whole wetting-and-drying cycle in mg (N) m^{-2} ; letters show significant difference ($p=0.05$, of log-transformed data); error bars indicate standard error of the mean of replicates (bare soil $n=3$; light BSC $n=4$; dark BSC $n=5$; chlorolichen BSC I $n=3$; chlorolichen BSC II $n=6$; moss BSC $n=4$).

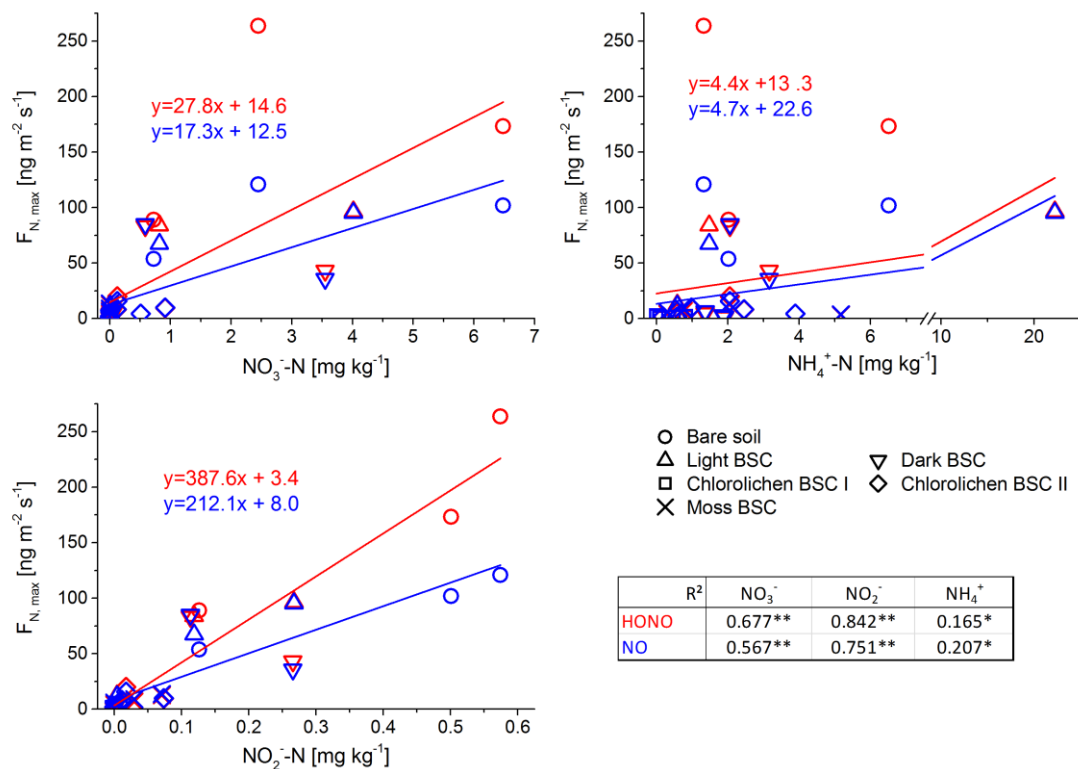


Fig. 6: Correlation between maximum flux of HONO and NO and nutrient content of all Cyprus soil and biocrust samples with Pearson correlation factors (of log transformed data; **: $p < 0.001$; *: $p < 0.05$).

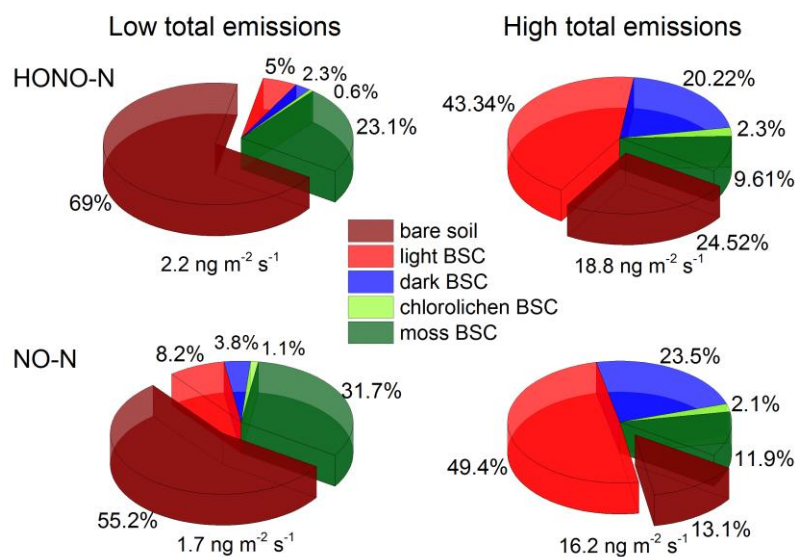
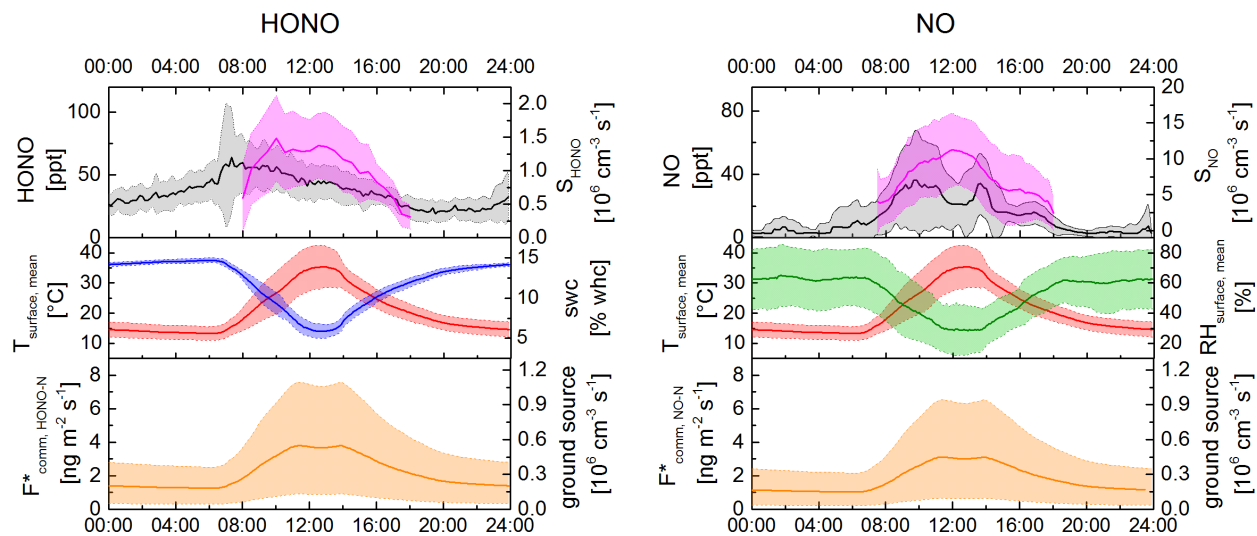


Fig. 7: Contributions of different ground surfaces to the total F^* .



Meusel et al., 2016 (CYPHEX 2014, wet period): — observed HONO or NO (stdev) — missing source of HONO or NO (stdev)
 Cyprus, April 2016: — mean surface Temperature (stdev) — mean surface RH (stdev) — estimated swc (stdev)
 — mean (min-max) F^* (left axis) or ground source (right axis)

Fig. 8: Diel pattern for HONO and NO emission in comparison with the observed HONO concentrations and missing source during the CYPHEX 2014 campaign. Upper panels: observed concentration of HONO and NO shown in black, missing source shown in pink. Middle panels: mean surface temperature and mean surface humidity measured in April 2016 in Cyprus and estimated soil water content shown in red, green and blue, respectively. Lower panel: calculated mean F^* (mean temperature) with the area indicating the lower and upper limit.